Simulation of the AGILE Gamma-Ray Imaging Detector Performance: Part II

Veronica Cocco [a,d], Francesco Longo [b,d], Marco Tavani [c,a,d]

[a] *Università degli Studi "Tor Vergata" and INFN Sezione di Roma II (Italy)*
[b] *Università degli Studi di Ferrara and INFN Sezione di Ferrara (Italy)*
[c] *Istituto di Fisica Cosmica, CNR, Milano (Italy)*
[d] *Consorzio Interuniversitario Fisica Spaziale, Torino (Italy)*

Abstract

In this paper (Paper II) we complete our discussion on the results of a comprehensive GEANT simulation of the scientific performance of the AGILE Gamma-Ray Imaging Detector (GRID), operating in the $\sim$ 30 MeV–50 GeV energy range in an equatorial orbit of height near 550 km. Here we focus on the on-board Level-2 data processing and discuss possible alternative strategies for event selection and their optimization.

We find that the dominant particle background components after our Level-2 processing are electrons and positrons of kinetic energies between 10 and 100 MeV penetrating the GRID instrument from directions almost parallel to the Tracker planes (incidence angles $\theta \gtrsim 90^\circ$) or from below.

The analog (charge) information available on-board in the GRID Tracker is crucial for a reduction by almost three orders of magnitude of protons (and heavier ions) with kinetic energies near 100 MeV.

We also present in this paper the telemetry structure of the GRID photon and particle events, and obtain the on-board effective area for photon detection in the energy range $\sim$ 30 MeV–50 GeV.

Key words: Gamma-ray Instruments, Montecarlo Simulation

1 Introduction

The use of solid state physics instruments for cosmic gamma-ray detection in space will substantially improve the scientific performance of high-energy astrophysics missions. AGILE [1,2] is a Small Scientific Mission supported by

the Italian Space Agency planned to be operational in 2003. AGILE is a relatively light instrument ($\sim$ 80 kg) based on state-of-the-art Silicon detector technology with excellent imaging capabilities in the gamma-ray (30 MeV–50GeV) and hard X-ray (10–40 keV) energy ranges. The Gamma-Ray Imaging Detector (GRID) is devoted to optimal detection and imaging of cosmic gamma-rays. It is basically made of a Silicon Tracker and a Mini-Calorimeter as described in Ref. [1]. The Silicon Tracker has 14 planes of Si microstrip detectors (121 μm pitch) with floating strip readout (readout pitch of 242 μm) for a total on-axis radiation length of 1 X_0. The Mini-Calorimeter, with a total on-axis radiation length of 1.5 X_0, supports the event energy determination and topological reconstruction of gamma-ray events.

In this paper we complete our analysis of the on-board data processing of cosmic photon and charged particle background events by what we define "Level-2/Step-1 data processing". We refer to a companion paper (Paper I, Longo, Cocco & Tavani, 2001) for details on the AGILE-GRID model and assumptions about the background and detector performance capabilities.

1.1 Summary of the GRID Level-1 data processing

As shown in Paper I the best Level-1 trigger strategy (required to be fast within a few tens of microseconds) is given by a combination of what we defined as the R11G and the DIS options. The R11G option is based on the combined use of signals from the anticoincidence (AC) panels and of the quantity R, defined as the ratio between the total number of hit TAA1 chips and the total number of fired X and Y views. The DIS option is a simplified track reconstruction based on computing the distance D of the fired TAA1s from the fired AC lateral panels.

From our simulations we showed that the R11G+DIS Level-1 trigger is quite efficient in rejecting $\sim 96\%$ of background charged particles without affecting significantly the cosmic gamma-ray detection [3]. Taking into account also the Earth albedo-photons, we expect a total (background plus cosmic photons) rate of $\lesssim$ 100 Hz after the hardware-implemented Level-1 trigger (see Paper I). This rate is consistent with the AGILE Data Handling (DH) processing requirements.

1.2 GRID Level-2 data processing

The two types of background events passing the Level-1 data processing are:

1) charged particle events due to primary and albedo protons, electrons and

positrons (average rate $\sim 70\,\mathrm{s}^{-1}$);
2) Earth albedo-photon events (average rate $\sim 20 - 40\,\mathrm{s}^{-1}$, depending on the instrument inclination with respect to the Earth surface).

After the Level-1 data processing, an additional event reduction is necessary on board to satisfy the GRID telemetry conditions. The goal is to achieve an event rate (comprehensive of cosmic gamma-rays and background events) of $\lesssim 30\,s^{-1}$. This Level-2 data processing and its implications are the main subjects of the current paper.

We distinguish two steps of Level-2 processing:

- Step-1: simple algorithms using cluster identification, analog information, and topology of events in the GRID Silicon Tracker (crucial for particle background rejection);
- Step-2: 3D-reconstruction algorithms aimed at determining the incoming photon directions (crucial for rejecting Earth albedo-photons).

In the following, we present the main results of the simulated charged particle background processing (Level-2/Step-1), and the requirements for the on-board Level-2 software to be applied to albedo-photons.

2 Level-2 Processing: Step-1

The Level-2 processing logic is applied after the Level-1 and Level-1.5 steps, and after the GRID data pre-processing, consisting in cluster identification and temporary storage in a GRID memory buffer. The Level-2 processing is asynchronous with respect to the real GRID data acquisition, and is typically limited to be completed within 1-2 milliseconds given the GRID background requirements. We assume R11G and DIS respectively as the Level-1 and Level-1.5 trigger steps; we define as "cluster" every group of consecutive fired Silicon strips with energy deposition larger than 27 keV (corresponding to 1/4 MIP [1]), and for every cluster we assume to have available from the on-board data processing the centroid (charge-barycentric) positions, cluster widths, and cluster total charges. An important factor to consider is the saturation of the GRID Silicon strip channels. When the energy release is larger than 5 MIP, the charge information saturates to its maximum value. Complete analog energy information is then available only for non-saturated strips, and we correctly simulate this hardware behavior.

Before discussing some Level-2 processing procedures, we recall the meaning

[1] MIP means Minimum Ionizing Particle energy release

of some quantities and Level-1 trigger steps defined in Paper I:

TRA = number of events characterized by primary particles or photons reaching the Tracker volume, a box of $38.06 \times 38.06 \times 21.078$ cm^3 which includes the Tracker planes from the top sheet of the first tungsten layer to the bottom sheet of the last Silicon-y plane;
PLA = events which give hits in at least 3 out of 4 consecutive planes (X OR Y view);
LAT = events passing the top-AC veto, with signals in 0 or 1 lateral AC panels, in 2 consecutive AC panels or in 2 AC panels on the same side;
R11G = LAT events with signals in 0 lateral AC panels, and LAT events with signals in 1 or 2 AC panels and $R > 1.1$;
DIS = simplified track reconstruction based on computing the distance D of the fired TAA1s from the fired AC lateral panel. The parameter DIS is defined as: $DIS = D_{fp} - D_{lp}$ where D_{fp} is the distance of the closest fired TAA1 to the fired AC lateral panel in the first plane, while D_{lp} is the distance of the closest fired TAA1 to the fired AC lateral panel in the last plane. We require $DIS \geq 0$ for good events. This option is applied only if there are fired AC lateral panels.

We discuss here four Level-2 processing procedures, some of them inspired by the corresponding Level-1 or Level-1.5 trigger options that successfully reject background particles without loosing too many cosmic gamma-ray photons:

1) **3PL:**
   is a condition more stringent than the PLA defined in Paper I; it requires hits on 3 consecutive planes (X AND Y views).
2) **CDIS:**
   is the application of the DIS algorithm to clusters instead of TAA1 chips. It is based on computing the distance CD of the clusters from the single fired AC panel. The parameter $CDIS$ is defined as $CDIS = CD_{firstplane} - CD_{lastplane}$ in order to have $CDIS \geq 0$ for good events (in case of a plane with more than one cluster, it is considered only the nearest cluster to the fired AC panel). This option is applied only if there are fired AC lateral panels.
3) **FCN3MIP:**
   this procedure is based on the use of the parameter $FCN = N_c(E > 3\,MIP)/N_{ctot}$ which is the fractional number of clusters with total energy larger than 3 MIPs (N_c), with N_{ctot} the total cluster number for the whole event; all events with $FCN > 0.6$ are rejected.
4) **M15**:
   The multiplicity M is the analogous of the ratio R, computed for clusters:
   M=(total number of clusters)/(total number of interested x/y views)
   The "M15 procedure" consists in rejecting all events with fired AC panels and with $M < 1.5$.

Tabs. 1, 2, 3 and Fig. 1 show the simulation results obtained applying the 3PL, CDIS, FCN3MIP and M15 procedures as Level-2 data processing steps applied in sequence. The particle and photon classes used in the simulations are the same used in Paper I. The suffix "TC" means "Tracker converted": only photons converted in the Tracker volume are "good photons", those for which there is good probability to reconstruct the incident direction.

We note that the 3PL procedure rejects events which are difficult to interpret, because of their "sparse" topology. This kind of events are typically produced by background electrons or positrons rather than by cosmic photons. The CDIS and M15 procedures follow the same philosophy of the Level-1.5 DIS option and of the Level-1 R11G option. The main difference is that they are applied to clusters instead of TAA1 chips, and therefore the spatial resolution is clearly better. The FCN3MIP procedure uses in a crucial way the GRID cluster analog information, and is very efficient in rejecting low-energy protons stopping in the Tracker volume. From Fig. 1 (upper panel, points marked with crosses) we note that the FCN3MIP procedure rejects low-energy protons by almost an order of magnitude, and has a very small effect on the rejection of cosmic off-axis gamma-rays (Fig. 1, lower panel). This is one of the most important results of our paper. Ionization losses of protons (or heavier nuclei) decelerating within the Tracker and eventually stopping inside it leave an unambiguous signature in terms of deposited charge in the Silicon microstrips. Our results on the proton background rejection are also clearly shown in Fig. 4, indicating a suppression by nearly one order of magnitude of the surviving flux from Level-1 to Level-2/Step-1 near kinetic energies of 100 MeV. At these energies, the total proton background suppression obtained on-board is by three orders of magnitude, by far the best results obtained by our background subtraction procedures. Our understanding of the particle background for an equatorial orbit of height near 550 km indicates that protons (and heavier nuclei) contribute about 10–20% of the total background rate of incident particles. An efficient rejection of this component is therefore very important.

We can conclude that simple Level-2 processing strategies can succeed in lowering the particle background rate from 70 s^{-1} to ~ 30 s^{-1} without affecting significantly the cosmic gamma-ray detection.

We extensively studied how the different trigger cuts modify the energy spectra and the angular distributions of the different background components. Figs. 2, 3 and 4 show the modifications of the charged particle background spectra and angular distributions due to Level-1, Level-1.5 and Level-2 data processing. Note that low-energy protons are rejected especially by the Level-2/Step-1 trigger selection and that most "surviving" particles are characterized by large values of the incidence angle ($\theta > 60^\circ$). This important qualitative feature of the surviving particle background applies also to electrons and positrons that constitute the majority of particles passing the Level-2/Step-1 processing. From Figs. 2 and 3 (lower panels) it is evident that particles penetrating in the GRID from below (with respect to the detector's Z-axis pointed in a direction opposite to that of the spacecraft) have a larger probability of passing the Level-2/Step-1 data processing. This conclusion is not surprising considering the shallowness of the Mini-Calorimeter and the existence of lateral GRID regions not covered by the Anticoincidence panels (Paper I). It is important to note that the AGILE-GRID will be an imaging gamma-ray instrument quite different from EGRET [4] that could discriminate against particles impinging on the detector from below because of a Time-of-Flight veto system. Background reduction for particles penetrating Silicon detectors similar to AGILE from below is a delicate matter, and needs to be addressed with great care.

Figs. 5 and 6 show the event selection and cuts for the albedo-photon spectra and their angular distributions for different GRID-Earth geometries. We base our analysis of Earth albedo photons on the simplified model described in Paper I. Fig. 5 refers to the case of the GRID pointing an unocculted portion of the sky with the Earth "below the GRID" and the direction towards the Earth center corresponding to the colatitude angle $\theta = 180^\circ$. Fig. 6 refers to the case of the Earth occulting approximately half of the GRID field of view. The most relevant feature of these albedo gamma-ray events is their large contribution to the total GRID background after the Level-2/Step-1 processing. Their differential spectra peak slightly below 10^3 $\mathrm{s}^{-1}\,\mathrm{GeV}^{-1}$ at photon energies near 10 MeV, and their total rate integrated over the whole spectrum is relatively high, of the same order as the surviving lepton rate (see Table 2). This result indicates the necessity of implementing on board an additional data processing for rejecting efficiently Earth albedo photons based on their incoming directions. This analysis goes beyond the scope of this paper and will be presented elsewhere.

In order to analyze the effect of the trigger selection on the cosmic gamma-ray photon spectrum and angular distribution we considered extragalactic cosmic gamma-rays with a power-law energy spectrum of index n=-2.1 and flux $\Phi(\mathrm{E} > 100\,\mathrm{MeV}) \simeq 10^{-5}\ \mathrm{ph\,cm^{-2}\,s^{-1}\,sr^{-1}}$ from Ref. [5], energies in the range 1 MeV $\div$ 100 GeV and directions in the ranges $\theta = 0^\circ - 180^\circ$, $\phi = 0^\circ - 360^\circ$. Fig. 7 shows the effects of trigger and processing cuts on the cosmic gamma-ray spectrum and angular distribution. We notice the excellent trigger performance of the GRID in terms of both spectral and angular responses. Trigger efficiency for photon detection and Level-2 successful processing varies between 15% and $\sim$ 40% depending on photon energy and direction.

3 Level-2 Processing: Step-2 and software requirements

The Earth albedo-photon component of the background is of great relevance. After the simplified processing of Level-1 and Level-2/Step-1, we can state the following:

a) the albedo photon background after Level-2/Step-1 is dominated by low-energy photons in the range $\sim 5\mathrm{MeV} < E < 30$ MeV, peaking at ~ 10 MeV.
b) the Level-2/Step-1 albedo photon event rate is near 20–30 s^{-1} and, when summed with the charged particle net rate, is too large to be sustained by the AGILE telemetry.

Therefore, the on-board background suppression requires further software data processing after the "simplified" Step-1 analysis presented in the previous section. We call this processing "Level-2/Step-2", aimed at an approximate but effective photon direction reconstruction. A detailed description of this Level-2 processing is beyond the scope of this paper, and it will be presented elsewhere.

4 GRID Telemetry

We summarize in this Section the main characteristics of the GRID scientific telemetry. Based on the selection cuts operated at Level-1 and Level-2 processing stages, we are in a position to assess the contribution to the scientific telemetry for both the particle and albedo-photon background and the cosmic gamma-ray signal.

It is crucial to realize that the number of bits N_{bits} generated by a typical "GRID event" is variable, depending on the number of Tracker clusters (N_{clus}), fired Mini-Calorimeter bars (N_{bars}) and other quantities (e.g.: N_{tplus}, the number of TAA1 chips exceeding the limit of 8 TAA1 for every 2 consecutive views). In the Montecarlo simulations we used the formula: $N_{bits} \simeq 176 + 29 \times N_{bars} + 57 \times N_{clus} + 9 \times N_{tplus}$, defining a "cluster" as a group of consecutive hit readout-strips with deposited charge $E > 1/4MIP$, and a "hit bar" every CsI bar with an energy release larger than $E = 0.7$ MeV. The considered formula represents the typical telemetry for GRID events. It takes into account the event header information and the main contributions of variable length. We emphasize that the assumed number of bits per cluster ($n = 57$) includes the total cluster width and deposited charge and all the analog information (position and deposited charge) that can be stored for 5 readout strips per cluster.

4.1 Telemetry event classes

The relevant components of the expected event rate after the Level-1 and the Level-2 trigger stages were simulated using the following event classes:

(A) **Electrons and positrons** (isotropic distributions), this class includes electron and positron classes described in Paper I;
(B) **Protons** (including primary and secondary components with proper angular distributions, AGILE pointing assumed to be with zenith angle $\theta = 0°$), this class includes low-energy proton and high-energy proton classes described in Paper I;
(C) **Earth albedo photons** (case ALB-1, unocculted AGILE's FOV, Earth below the Tracker), this class is the same considered in Paper I;
(D) **Cosmic gamma-rays** (extragalactic diffuse emission), this class was described in Sect. 2.3 of this paper.

Since the average number of bits per GRID event strongly depends on the particle/photon energy and inclination and since gamma-rays above hundreds of MeV constitute a very important component of the scientific data, we considered also the high-energy and very high-energy photon classes summarized in Tab. 5.

4.2 Simulation results

Simulation results are summarized in Tab. 6. We find that the lepton component of the background is expected to dominate the GRID scientific telemetry. We note that the lepton surviving the current Level-2 cuts are dominated by

low-energy events ($E \sim 20 - 30$ MeV) with characteristics similar to those of cosmic low-energy gamma-rays. The typical telemetry load for these low-energy leptons is below 1.5 kbit/event. Low-energy protons are efficiently rejected by the Level-1 and Level-2/Step-1 logic. Note that the telemetry distributions of photon classes are biased towards the low-energy photons. The average number of bits per GRID event strongly depends on the photon energy and inclination.

In principle, each particle and photon event is characterized by different GRID topologies, and therefore different telemetry loads. However, in practice all particle/photon components passing the Level-2 processing have quite similar N_{bits} distributions, as shown by Fig. 8. All distributions peak near or below 1 kbit/event with average numbers given in Tab. 6.

5 GRID Effective Area

The effective area is, by definition, $A_{eff} = \epsilon A_{\perp}$, where $A_{\perp}$ is the detector "geometrical area" (equivalent area perpendicular to the incident flux direction) and ϵ is the detector efficiency. The detector efficiency is given by the photon interaction probability (ϵ_i) times the trigger efficiency (ϵ_t) times the track reconstruction efficiency (ϵ_r): $\epsilon = \epsilon_i \cdot \epsilon_t \cdot \epsilon_r$.

Track reconstruction (implying a reliable vertex identification and direction reconstruction) is strongly influenced by the event topologies. Taking into account average properties of the events, we assumed in Fig. 10 the following values: $\epsilon_r = 1$ for $E > 25$ MeV and $\epsilon_r = 0.75$ for $E = 25$ MeV.

The value of $\epsilon_i \cdot \epsilon_t$ is given by the following ratio: $\epsilon_i \cdot \epsilon_t$ = N(M15_TC)/N(TRA_TH) since "good photons" are only the ones that pass the Level-2 trigger (R11G+DIS +M15) having converted in the tracker volume, and they must be compared with the total number of photons that would geometrically enter the tracker volume. N(TRA_TH) can be evaluated theoretically as N(TRA_TH) = $F \cdot A_{\perp}$, where F is the photon incident flux, which is related to the total number of events generated on the spherical surface around the detector by the relation $F = N_{TOT}/(\pi\, r^2)$, where r is the sphere radius (we generally use r=89 cm and $N_{TOT} = 50000$).

In order to study the GRID effective area we considered on-axis photons ($\theta = 0°$, $\phi = 0°$) and photons with $\theta = 50°$ and $\phi = 0°$, with the following energies: E= 25 MeV, 100 MeV, 1 GeV, 10 GeV, 50 GeV. Fig. 9 provide information on how the event cuts adopted in this document affect the GRID gamma-ray detection. The processing steps adopted by Level-1.5 and Level-2/Step-1 are crucial in lowering the particle background rate from $\sim 120\,\mathrm{s}^{-1}$ (after R11G)

to $\sim 30\,\mathrm{s}^{-1}$ (after Level-2/Step-1). However, these event cuts also cause a decrease of the effective area, especially for off-axis photons. Fig. 10 shows the comparison among AGILE, EGRET and COMPTEL effective areas, for fixed directions, as a function of photon energy.

6 Conclusions

The trigger and processing strategy presented in this paper to filter and select particle and photon GRID events can be summarized as follows.

Events induced by electrons and positrons constitute the main background component and dominate the scientific telemetry of the AGILE-GRID. The total lepton event rate obtained for the trigger and processing strategy presented in this paper (Level-2/Step-1 processing) is $R_{e^+/e^-} \simeq 30\ \mathrm{s}^{-1}$. A goal of the Level-2/Step-2 processing through a three-dimensional photon direction reconstruction is to further reduce this background component by almost a factor of 2, reaching $R_{e^+/e^-}(\text{required rate}) \leq 15\ \mathrm{s}^{-1}$.

Earth albedo gamma-ray photons after the Level-2/Step-1 processing produce an event rate $R_{albedo-\gamma} \simeq 20 - 30\ \mathrm{s}^{-1}$, depending on the geometry and comparable to that of leptons. This event rate is too large to be acceptable by the AGILE telemetry, and further reduction of this component is necessary. A 3D-direction reconstruction algorithm to be implemented by the Level-2/Step-2 processing is required to reduce this rate at least by a factor of 10, reaching the telemetry rate requirement: $R_{albedo-\gamma}(\text{required rate}) \leq 3\ \mathrm{s}^{-1}$.

Low-energy proton events ($E_{kin} < 400$ MeV) are efficiently decreased by the on-board Level-1 and Level-2 logic, especially because of the available Si strip analog information. High energy protons (of energy near or larger than 1 GeV) tend to dominate the telemetry of proton events. The simulated Level-2/Step-1 processing of protons produce an event rate near the required value, $R_{protons}(\text{required rate}) \leq 1\ \mathrm{s}^{-1}$.

At the end, the event rate for cosmic gamma-ray events, the scientific signal of the AGILE-GRID, turns out to be ~ 100 times smaller than the (lepton, proton, albedo-photon) background after the Level-2/Step-1 processing. As required by our strategy, cosmic gamma-rays are quite efficiently detected and filtered by the on-board GRID data processing, reaching optimal detection efficiency near 100 MeV.

We notice that a substantial number of cosmic photon events passing the Level-2 processing have energies between 10 MeV and 30 MeV, as it can be deduced from Fig. 7. Table 7 summarizes our conclusions.

7 Acknowledgments

Results presented in this paper are based on joint work with members of the AGILE Team. In particular, we thank G. Barbiellini, P. Picozza, A. Morselli and the AGILE Simulation and Theory Group for many discussions and support.

The current work was carried out at the University of Rome "Tor Vergata", University of Ferrara and CNR and INFN laboratories under the auspices and partial support of the Agenzia Spaziale Italiana.

References

[1] Tavani, M., et al., 2001, *Science with AGILE*, AGILE Internal Note, A-P-019; http://www.ifctr.mi.cnr.it/Agile.

[2] Tavani, M., et al., 2001, invited paper presented at the *Gamma 2001 Symposium*, Baltimore, 4-6 April 2001, to be published by the American Institute of Physics Conference Proceedings.

[3] Longo, F., Cocco, V. & Tavani, M., 2001, submitted to NIM (Paper I).

[4] Thompson, D.J., et al., 1993, Astrophys. J. Supp., 86, 629.

[5] Sreekumar, P., et al., 1998, Astrophys. J., 494, 523.

[6] Vercellone, S., et al., 2001, in *Probing the Physics of Active Galactic Nuclei by Multiwavelength Monitoring*, NASA-GSFC Greenbelt 2000, eds. B.M. Peterson, R.S. Polidan & R.W. Pogge, ASP Conf. Series 224, p.483-490.

[7] Thompson, D.J., et al., 1993, Astrophys. J. Supp., 86, 629.

[8] Schoenfelder V., et al., 1993, Astrophys. J. Supp., 86, 657.

FIGURE CAPTIONS:

Fig.1: Efficiency of the GRID Level-2/Step-1 data processing in rejecting particle background events (upper panel) and in detecting photons (lower panel). The suffix "TC" means "Tracker converted" (only photons converted in the Tracker volume have been considered) and "FCN_TC" means "FCN3MIP_TC" (see text).
Fig.2: Simulated differential energy (upper panel) and angle (lower panel) distributions resulting from the processing of the electron background by the

AGILE-GRID on-board Data Handling. The upper solid curve represents the particles above 10 MeV penetrating into the Tracker volume (TRA). The long-dashed curve and the dot-dashed curves refer to the Level-1 processing (PLA and R11G), respectively. The short dashed curve refers to the Level-1.5 processing (DIS). The thick solid curve represents the particle flux passing the sequence of Level-2/Step-1 data processing (indicated with M15).
Fig.3: Simulated differential energy (upper panel) and angle (lower panel) distributions resulting from the processing of the positron background by the AGILE-GRID on-board Data Handling. The upper solid curve represents the particles above 10 MeV penetrating into the Tracker volume (TRA). The long-dashed curve and the dot-dashed curves refer to the Level-1 processing (PLA and R11G), respectively. The short dashed curve refers to the Level-1.5 processing (DIS). The thick solid curve represents the particle flux passing the sequence of Level-2/Step-1 data processing (indicated with M15).
Fig.4: Simulated differential energy (upper panel) and angle (lower panel) distributions resulting from the processing of the proton background by the AGILE-GRID on-board Data Handling. The upper solid curve represents the particles above 10 MeV penetrating into the Tracker volume (TRA). The long-dashed curve and the dot-dashed curves refer to the Level-1 processing (PLA and R11G), respectively. The short dashed curve refers to the Level-1.5 processing (DIS). The thick solid curve represents the particle flux passing the sequence of Level-2/Step-1 data processing (indicated with M15).
Fig.5: Simulated differential energy (upper panel) and angle (lower panel) distributions resulting from the processing of the Earth albedo-photon (ALB-1, see text for definition) background by the AGILE-GRID. The upper solid curve represents the photons above 1 MeV penetrating into the Tracker volume (TRA). The long-dashed curve and the dot-dashed curves refer to the Level-1 processing (PLA and R11G), respectively. The short dashed curve refers to the Level-1.5 processing (DIS). The thick solid curve represents the photon flux passing the sequence of Level-2/Step-1 data processing (indicated with M15).
Fig.6: Simulated differential energy (upper panel) and angle (lower panel) distributions resulting from the processing of the Earth albedo photon (ALB-2, see text for definition) background by the AGILE-GRID. The upper solid curve represents the photons above 1 MeV penetrating into the Tracker volume (TRA). The long-dashed curve and the dot-dashed curves refer to the Level-1 processing (PLA and R11G), respectively. The short dashed curve refers to the Level-1.5 processing (DIS). The thick solid curve represents the photon flux passing the sequence of Level-2/Step-1 data processing (indicated with M15).
Fog.7: Simulated differential energy (upper panel) and angle (lower panel) distributions from the processing of cosmic extragalactic gamma-rays by the AGILE-GRID. The upper solid curve represents the photons above 1 MeV penetrating into the Tracker volume (TRA). The long-dashed curve and the dot-dashed curves refer to the Level-1 processing (PLA and R11G), respec-

tively. The short dashed curve refers to the Level-1.5 processing (DIS). The thick solid curve represents the photon flux passing the sequence of Level-2/Step-1 data processing (indicated with M15).
Fig.8: Telemetry distributions (N_{bits}/event) normalized to unity. *Continuous line:* electron-positron component; *Dashed line:* proton component; *Dotted line:* albedo gamma-ray component; *Dashed-dotted line:* extragalactic diffuse gamma-rays.
Fig.9: Comparison between the AGILE-tracker effective area obtained applying only R11G Level-1 Trigger and the AGILE-tracker effective area obtained applying M15 Level-2 Trigger (after R11G+DIS).
Fig.10: AGILE, EGRET and COMPTEL effective areas after track reconstruction. Figure adapted from Refs.[1,6]. EGRET and COMPTEL data are from Refs.[7,8].

Table 1
Level-2/Step-1 processing effects on Background Charged Particles

	ELE (s^{-1})	POS (s^{-1})	HE PROT (s^{-1})	LE PROT (s^{-1})	TOTAL (s^{-1})
R11G	55	54	4.1	6.2	**119**
DIS	35	30	1.5	3.4	**70**
3PL	28	25	1.4	3.1	58
CDIS	25	22	1.1	2.9	51
FCN3MIP	23	21	0.8	0.6	45
M15	13	14	0.7	0.5	**28**

Table 2
Level-2/Step-1 processing effects on Background Albedo Photons

	ALB-1 PHOT (s^{-1})	ALB-2 PHOT (s^{-1})
R11G	22	40
DIS	20	39
3PL	16	30
CDIS	15	29
FCN3MIP	15	27
M15	15	26

Table 3
Level-2/Step-1 processing effects on Cosmic Gamma-Rays (*)

Photons	HE 0-10	HE 50-60	LE 0-10	LE 50-60
R11G_TC	40%	26%	26%	18%
DIS_TC	39%	25%	26%	17%
3PL_TC	39%	25%	25%	16%
CDIS_TC	38%	24%	24%	16%
FCN3MIP_TC	38%	23%	24%	15%
M15_TC	37%	21%	24%	14%

(*) We reported the detection efficiencies: the percentages of selected events respect to the total number of photons that theoretically could enter into the Tracker volume (% of TRA_TH, as defined in Paper I).

Table 4
GRID background rates after Level-2/Step-1 processing

Background component	unocculted GRID FOV	half-occulted GRID FOV
Charged particles	30 s^{-1}	30 s^{-1}
Earth albedo photons	20 s^{-1}	30 s^{-1}
Total	50 s^{-1}	60 s^{-1}

Table 5
Photon classes

Class	E_{kin}^{min}	E_{kin}^{MAX}	Energy Spectrum	θ	ϕ
HE 0-10	400 MeV	1 GeV	Power-law (n=-2)	$0^\circ \div 10^\circ$	$0^\circ \div 360^\circ$
HE 50-60	400 MeV	1 GeV	Power-law (n=-2)	$50^\circ \div 60^\circ$	$0^\circ \div 360^\circ$
VHE 0-10	1 GeV	100 GeV	Power-law (n=-2)	$0^\circ \div 10^\circ$	$0^\circ \div 360^\circ$
VHE 50-60	1 GeV	100 GeV	Power-law (n=-2)	$50^\circ \div 60^\circ$	$0^\circ \div 360^\circ$

Table 6
Average and maximum bit number for different event classes

Event class	Average N_{bits}	Maximum N_{bits}
Electrons/positrons	1.4 kbit	5.0 kbit
Protons	1.7 kbit	5.0 kbit
Earth albedo photons	1.0 kbit	3.0 kbit
Cosmic gamma-rays	1.1 kbit	4.0 kbit
PHOT HE 0-10	2.5 kbit	6.5 kbit
PHOT HE 50-60	2.5 kbit	7.0 kbit
PHOT VHE 0-10	2.6 kbit	7.0 kbit
PHOT VHE 50-60	3.1 kbit	8.5 kbit

Table 7
AGILE-GRID Telemetry Summary

Component	Event Rate (s^{-1}) (this work)	Rate Req. (s^{-1}) (Level-2/Step-2)	$\frac{<N_{bits}>}{event}$	$< N_T >$/orbit (1 orbit=5400 sec)
Leptons	30	≤ 20	1.4 kbit	$\leq$ 151 Mbit
Protons	1	≤ 1	1.7 kbit	$\leq$ 9 Mbit
Albedo γ's	20–30	≤ 3	1.0 kbit	$\leq$ 16 Mbit
Cosmic γ's	0.1–1	0.1–1	1.1 kbit	(0.6–6) Mbit
Total				182 Mbit

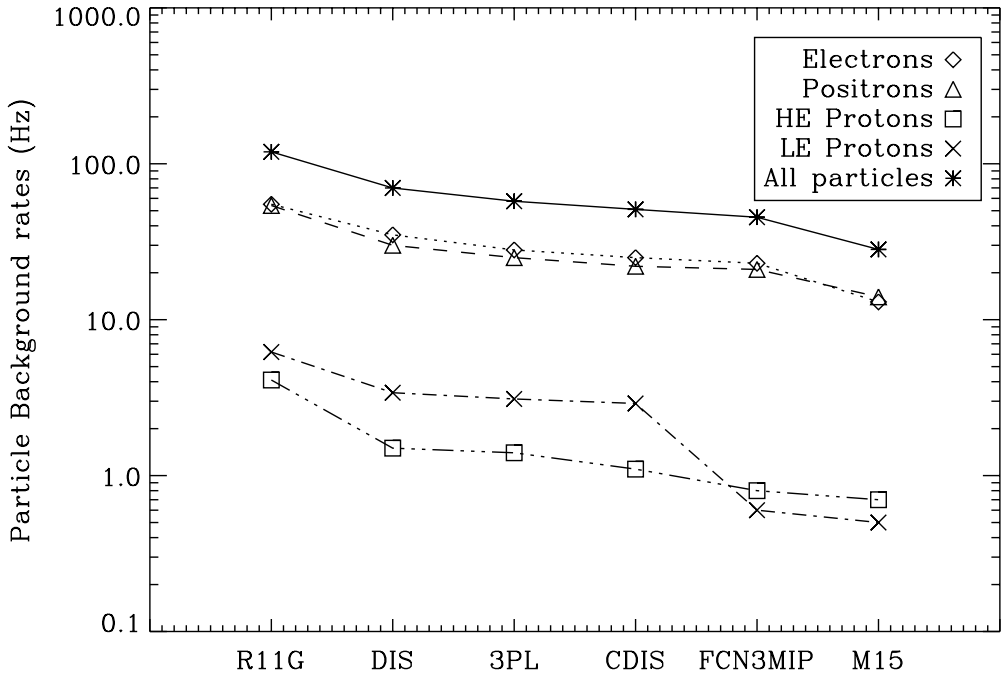
Particle Background rates (Hz)
1000.0
100.0
10.0
1.0
0.1
Electrons
Positrons
HE Protons
LE Protons
All particles
R11G
DIS
3PL
CDIS
FCN3MIP
M15

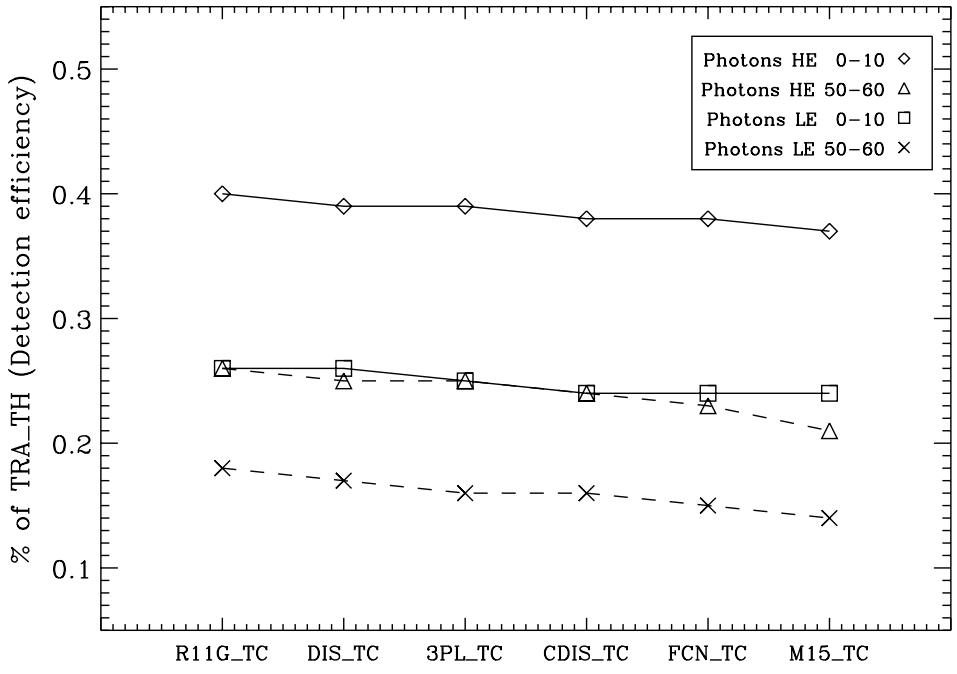
% of TRA_TH (Detection efficiency)
0.5
0.4
0.3
0.2
0.1
Photons HE 0-10
Photons HE 50-60
Photons LE 0-10
Photons LE 50-60
R11G_TC
DIS_TC
3PL_TC
CDIS_TC
FCN_TC
M15_TC

Fig. 1.

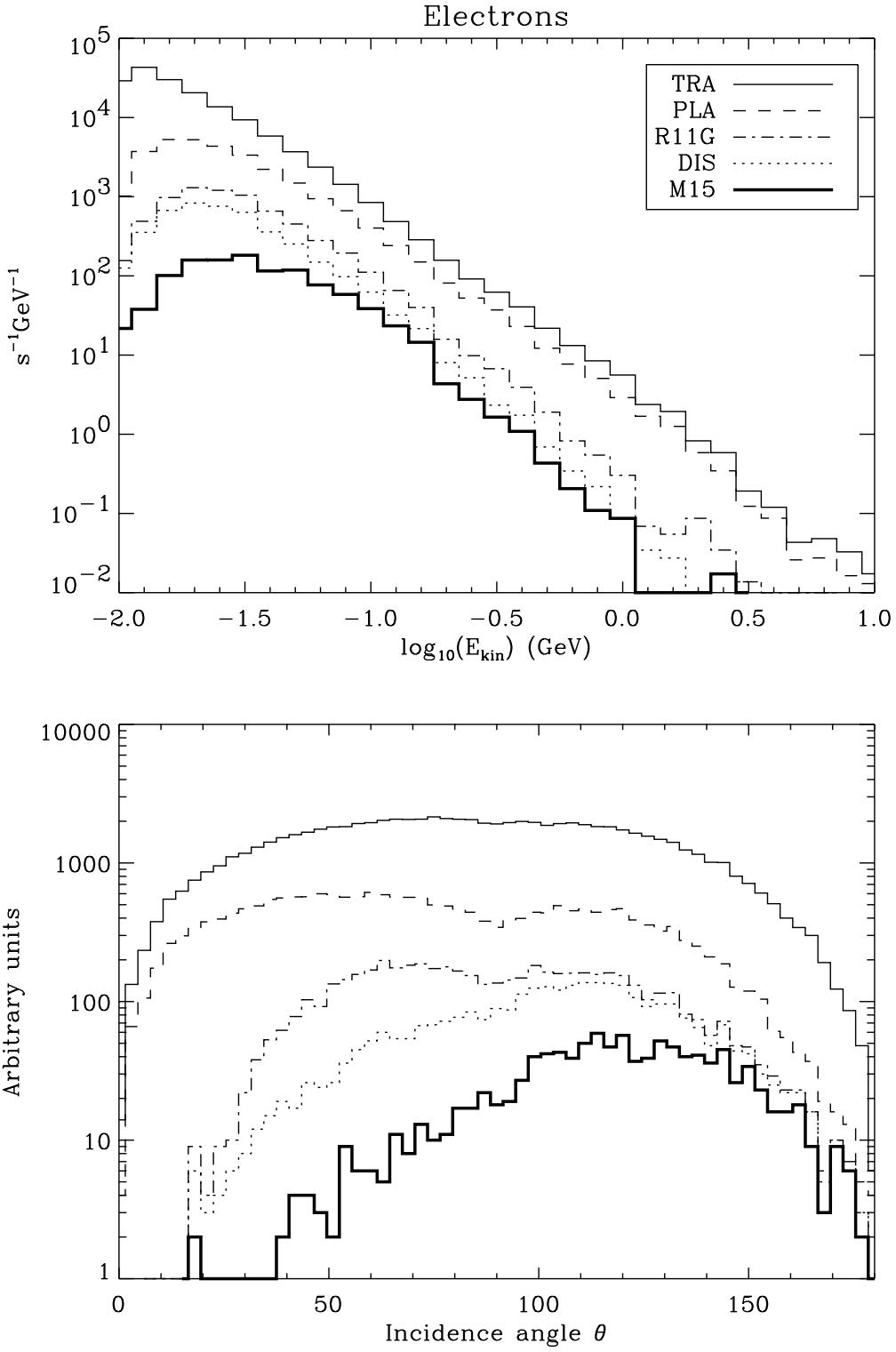
Electrons
TRA
PLA
R11G
DIS
M15
10^5
10^4
10^3
10^2
10^1
10^0
10^{-1}
10^{-2}
$s^{-1}GeV^{-1}$
−2.0
−1.5
−1.0
−0.5
0.0
0.5
1.0
$\log_{10}(E_{kin})$ (GeV)
10000
1000
100
10
1
Arbitrary units
0
50
100
150
Incidence angle θ

Fig. 2.

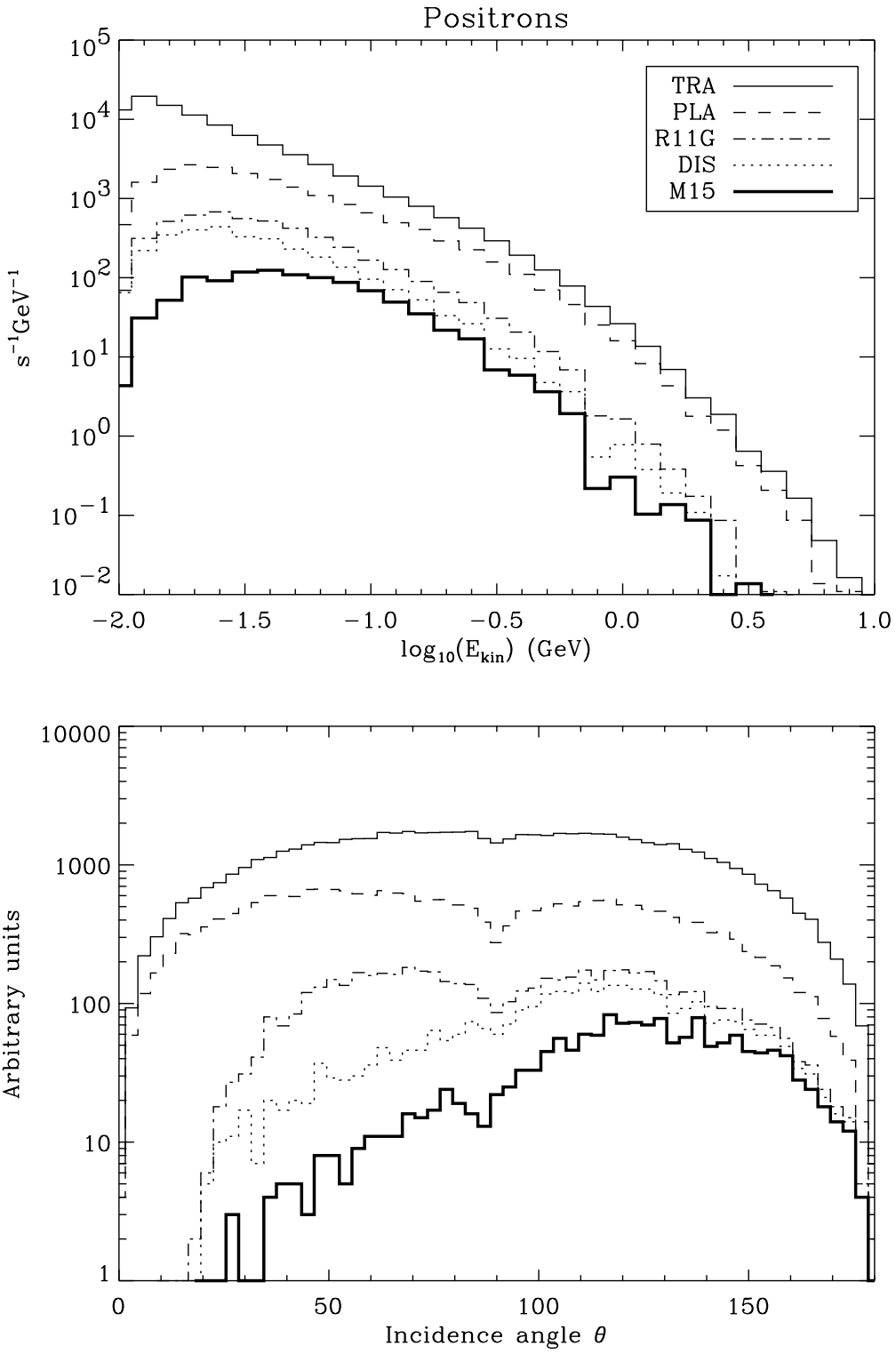
Positrons
TRA
PLA
R11G
DIS
M15
$s^{-1}GeV^{-1}$
$\log_{10}(E_{kin})$ (GeV)
Arbitrary units
Incidence angle θ

Fig. 3.

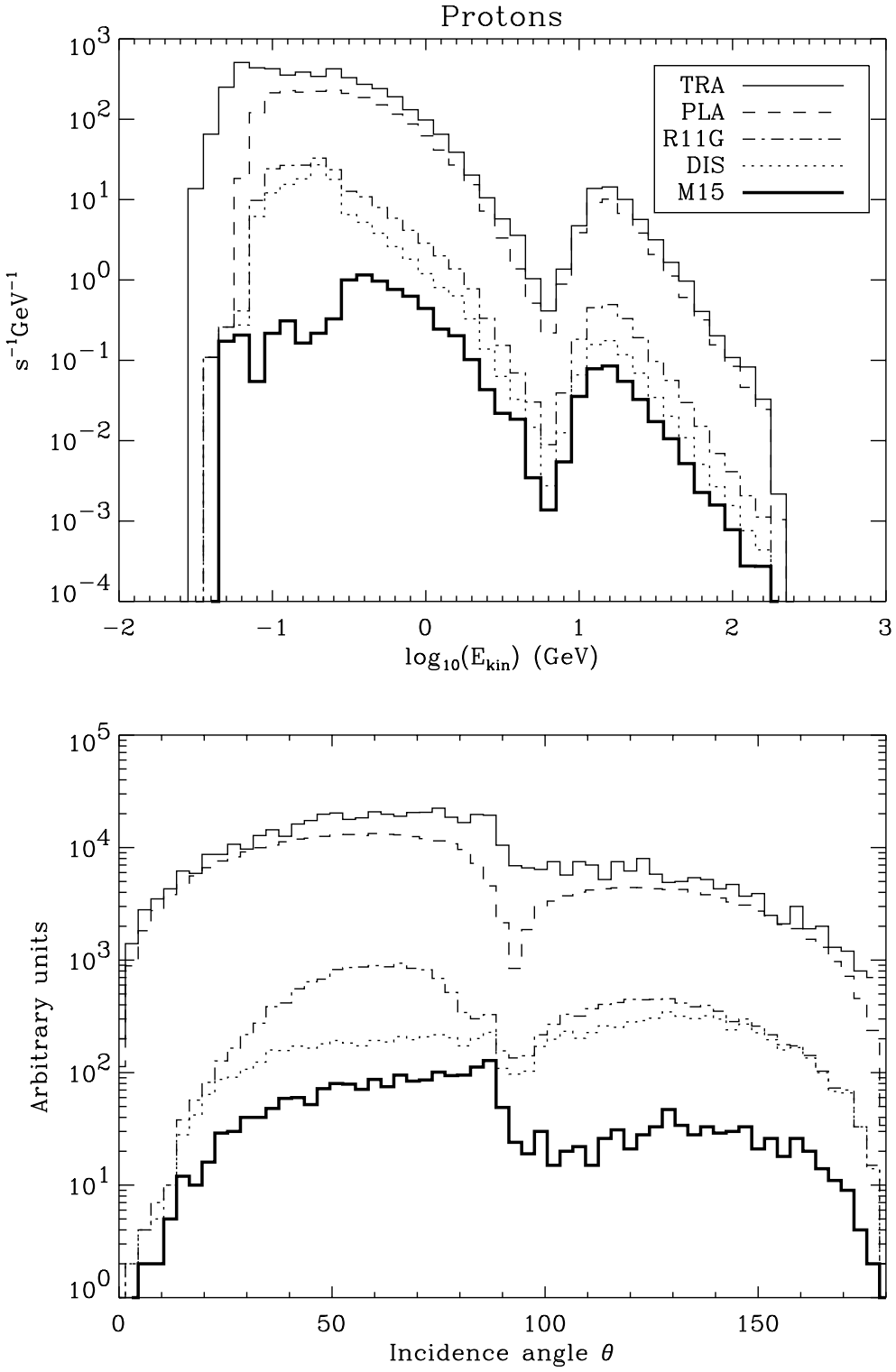
Protons
TRA
PLA
R11G
DIS
M15
$s^{-1}GeV^{-1}$
$\log_{10}(E_{kin})$ (GeV)
Arbitrary units
Incidence angle θ

Fig. 4.

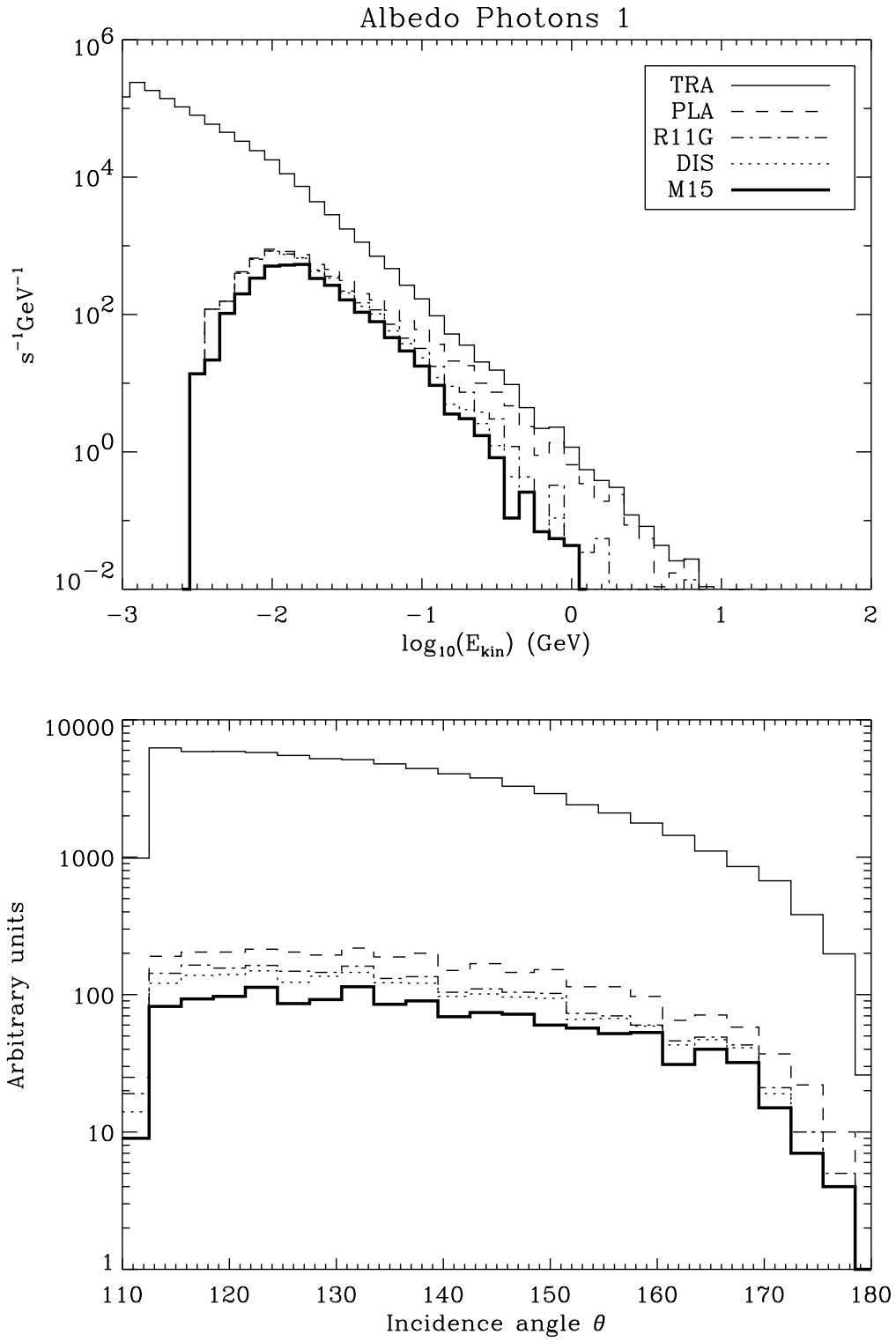
Albedo Photons 1
TRA
PLA
R11G
DIS
M15
10^6
10^4
10^2
10^0
10^{-2}
$s^{-1}GeV^{-1}$
−3
−2
−1
0
1
2
$\log_{10}(E_{kin})$ (GeV)
10000
1000
100
10
1
Arbitrary units
110
120
130
140
150
160
170
180
Incidence angle θ

Fig. 5.

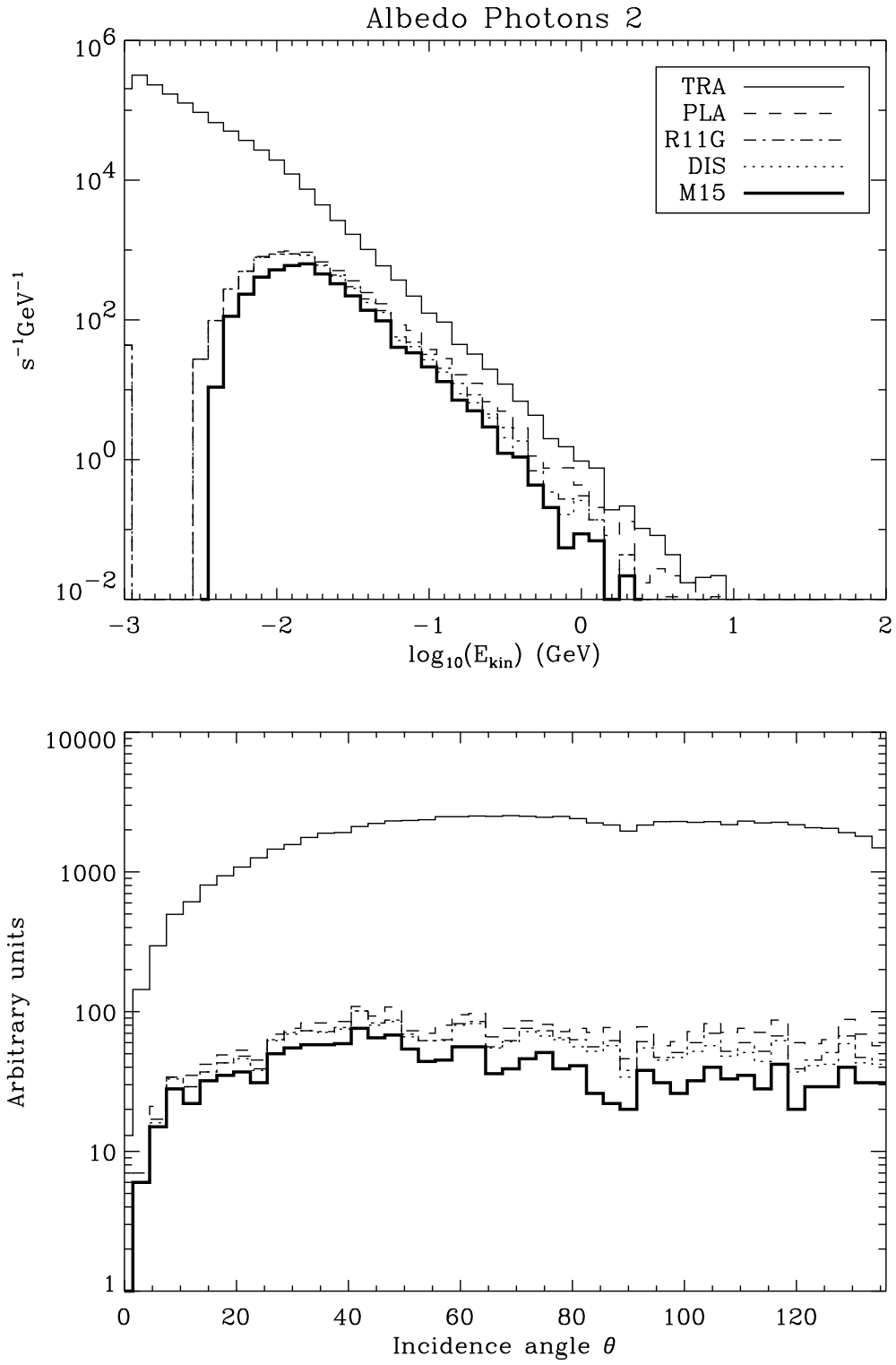
Albedo Photons 2
TRA
PLA
R11G
DIS
M15
10^6
10^4
10^2
10^0
10^{-2}
$s^{-1}GeV^{-1}$
−3
−2
−1
0
1
2
$\log_{10}(E_{kin})$ (GeV)
10000
1000
100
10
1
Arbitrary units
0
20
40
60
80
100
120
Incidence angle θ

Fig. 6.

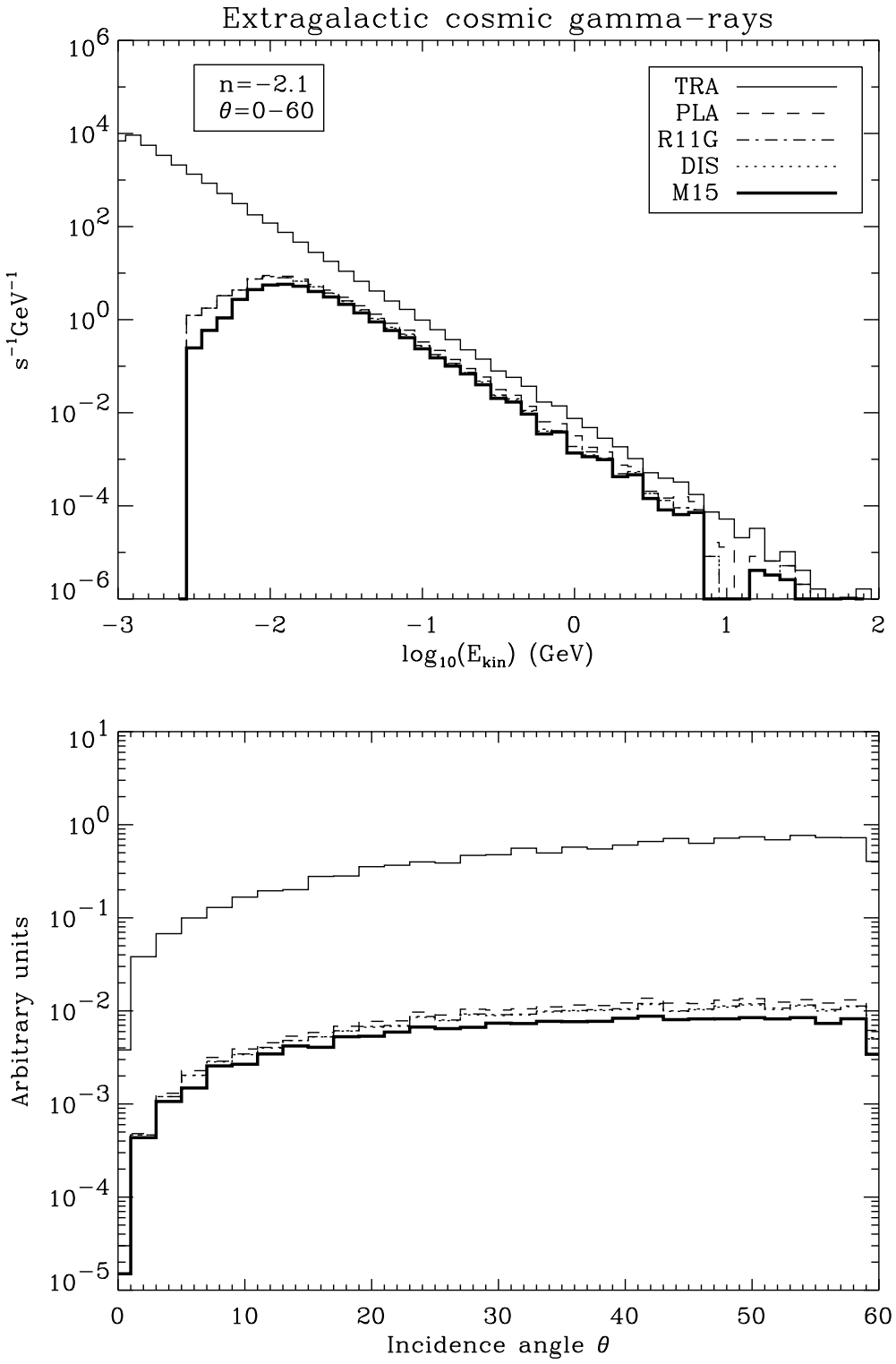
Extragalactic cosmic gamma−rays
n=−2.1
θ=0−60
TRA
PLA
R11G
DIS
M15
s⁻¹GeV⁻¹
log10(Ekin) (GeV)
Arbitrary units
Incidence angle θ

Fig. 7.

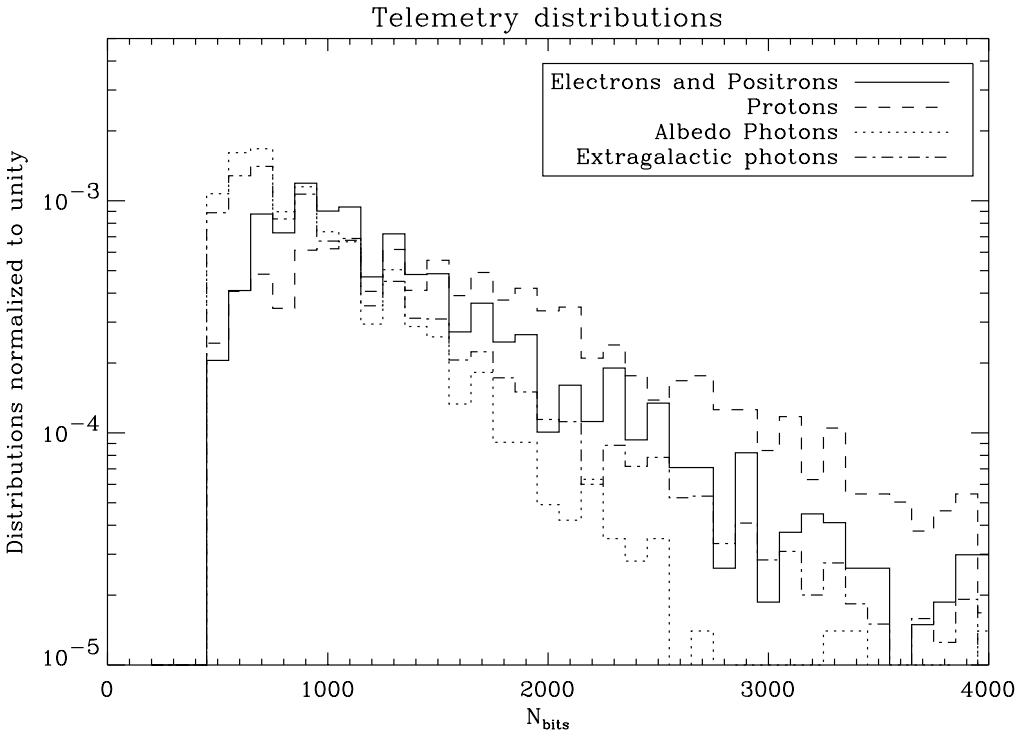
Telemetry distributions
Electrons and Positrons
Protons
Albedo Photons
Extragalactic photons
Distributions normalized to unity
10^{-3}
10^{-4}
10^{-5}
0
1000
2000
3000
4000
N_{bits}

Fig. 8.

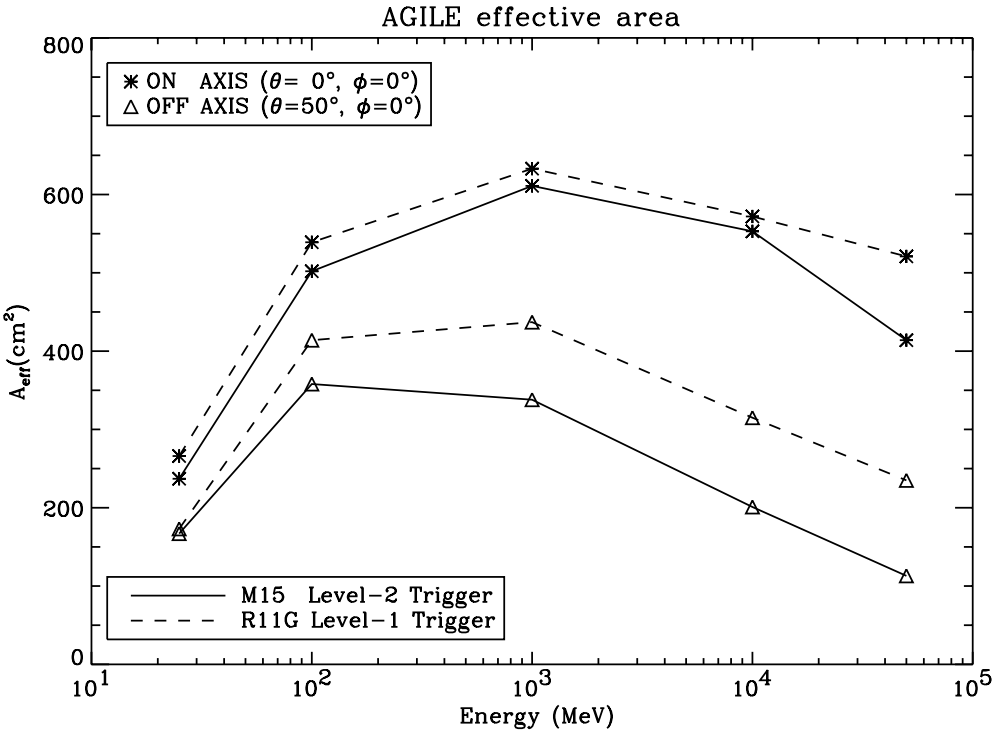
AGILE effective area
✱ ON AXIS (θ= 0°, ϕ=0°)
△ OFF AXIS (θ=50°, ϕ=0°)
M15 Level−2 Trigger
R11G Level−1 Trigger
$A_{eff}(cm^2)$
800
600
400
200
0
10^1
10^2
10^3
10^4
10^5
Energy (MeV)

Fig. 9.

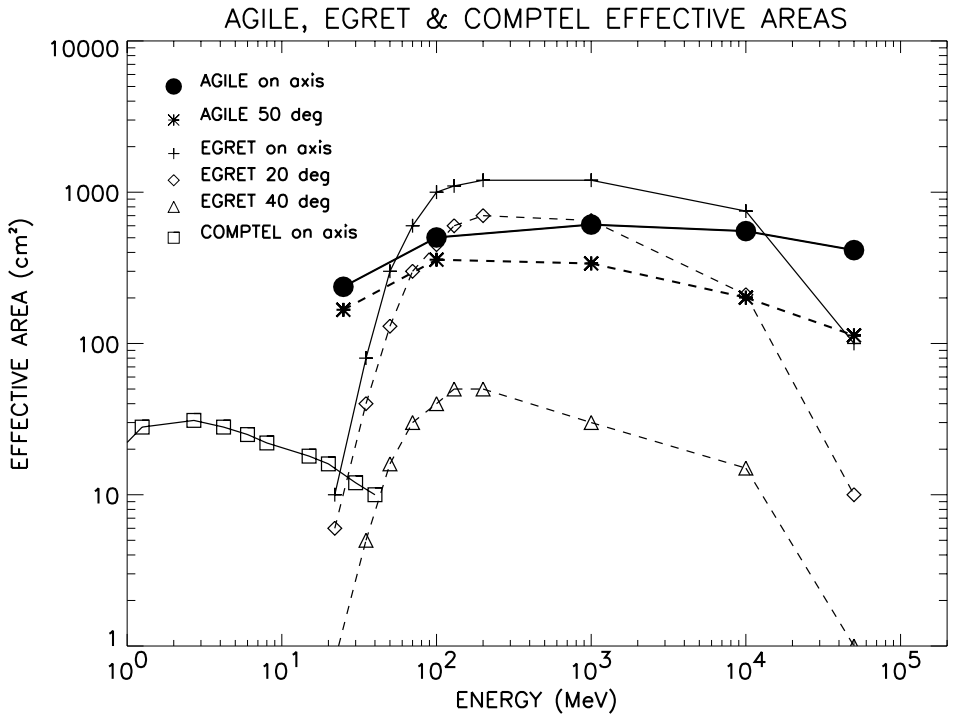
AGILE, EGRET & COMPTEL EFFECTIVE AREAS
AGILE on axis
AGILE 50 deg
EGRET on axis
EGRET 20 deg
EGRET 40 deg
COMPTEL on axis
EFFECTIVE AREA (cm²)
ENERGY (MeV)
10000
1000
100
10
1
10^0
10^1
10^2
10^3
10^4
10^5

Fig. 10.